Scientific Herald of Uzhhorod University
Series "Physics"

Journal homepage: https://physics.uz.ua/en
Issue 51, 30-38
Received: 07.04.2022. Revised: 22.05.2022. Accepted: 10.06.2022

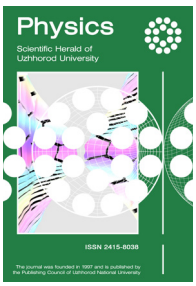

UDC 539.125
PACS 29
DOI: 10.54919/2415-8038.2022.51.30-38

A Simple Model for Describing the Minimum Differential Cross-Section of Elastic Proton Scattering on Protons at High Energies

Norbert Bence[1], Alexander Lengyel[2], Zoltán Tarics[2*]

[1]Uzhhorod National University

88000, 14 Universitetska Str., Uzhhorod, Ukraine

[2]Institute of Electron Physics of the NAS of Ukraine

88017, 21 Universytetska Str., Uzhhorod, Ukraine

Abstract

Relevance. The most modern and widely applied phenomenological theory, which well describes an entire range of physical characteristics of such processes as elastic and inelastic proton-proton and antiproton-proton scattering at high energies, is the Regge poles method in relativistic theory. Based on a simple amplitude, such as the dipole pomeron, where the pomeron is the Regge pole, the researchers add different terms to it. Using such more complex amplitudes, it is possible to explain well or satisfactorily together not only the experimental data for these reactions obtained at the end of the last century, but also the latest ones obtained at the Large Hadron Collider.

Purpose. The purpose of this study is to find numerical values of the amplitude parameters at which the vicinity of minimum of the differential cross-sections of elastic proton scattering on protons at high energies are satisfactorily described, and to answer whether the parameters satisfy the obtained constraints.

Methods. To find the amplitude parameters, the least squares method is used and minima equations are obtained for the squares of differences between the experimental and theoretical values of these cross-sections. These equations are transcendental, and therefore, they are solved by approximation. Within the framework of successive approximations, a method is selected that ensures fast convergence of the process, namely: the faster descent method or the gradient method. Parameter errors are calculated using a covariance matrix. The statistical acceptability of the model is determined according to the Fischer criterion.

Results. Numerical calculations from experimental data of differential cross-sections of elastic *pp*-scattering were used to find the values of the parameters and the scale multiplier of the amplitude. Differential cross-sections are calculated from the amplitude near the minima. The corresponding graphs of these cross-sections are presented. The coincidence with the experiment is satisfactory in most cases, and in some cases, it is of high quality. A covariance matrix is obtained, from which the errors of the model parameters are found. Under general conditions, restrictions on the found approximate values of parameters are derived. It is shown that they satisfy the constraint. According to the Fischer criterion, the statistical acceptability of the model was verified, which turned out to be positive.

Conclusions. The proposed simple amplitude ensures that the Froissart constraint and unitarity are met. It will serve as a seed for constructing more complex amplitudes that will describe a wide range of experiments on proton-proton and antiproton-proton scattering at high energies

Keywords: amplitude, parameter, dipole pomeron, covariance matrix

Suggested Citation:
Bence N, Lengyel A, Tarics Z. A simple model for describing the minimum differential cross-section of elastic proton scattering on protons at high energies. *Scientific Herald of Uzhhorod University. Series "Physics"*. 2022;(51):30-38.

*Corresponding author

Introduction

Regge's theory of complex angular moments in quantum mechanics, which is generalised to relativistic S-matrix in terms of Mandelstam variables, which has been developed for more than 50 years and is used to explain experimental results obtained in processes implemented in high-energy collisions of elementary particles. This primarily concerns pp- and $\bar{p}\,p$-scattering both elastic and inelastic. Over the past 10 years, on the Large Hadron Collider has been obtained data on differential cross-sections (and not only) of the elastic pp-scattering at several energies [1-3]. Measurements at the Collider when two protons collide with a total energy of 7 TeV [2] in the centre of mass system turned out to be decisive, since they were the first experiment after launching the accelerator and showed the potential of the detector.

Phenomenological models of Regge require complex amplitudes containing many terms and even more parameters to describe a large database of experimental data on the total and differential sections, the slope, and curvature parameter of the last section, and the ratio of the real part of the amplitude to its imaginary one at zero transferred momentum. For example, to describe the total cross-section of scatterings in a wide energy region, socalled reggeones are introduced, i.e., f- and ω-mesons, nonlinear trajectories with the intersept larger than 1 [4]. Adding such terms to the amplitude means that 6 added parameters appear. To explain more physical quantities in wide areas of variables, one needs to add other terms: introduce a tripole pomeron, odderon [5-7]. Even more parameters need to be considered if the spin structure of the amplitude is factored [5; 8; 9].

Most models that simultaneously explain the physical quantities listed above necessarily contain in the amplitude the pomeron [4; 10] (and possibly odderon), its trajectory, i.e., they take such a primitive amplitude as a basis. The simplest one includes a dipole pomeron, and it corresponds to the first degree lns, where s is the square of the energy of protons in the system of their centre of mass. The tripole pomeron corresponds to ln^2s, etc.

Keeping in mind the optical theorem that relates the amplitude to the total cross-section, instead of the amplitude as a sum in degrees of logarithm, an expression for the total cross-section of the process can be written. However, the already tripole pomeron violates the unitarity of the theory, which is often ignored in numerical calculations, considering that the current high energies are far from asymptotically large, where this violation becomes noticeable. To restore unitarity, as a rule, the amplitude over which the so-called eikonal transformation is performed is used [11; 12].

In this paper, the authors investigate the simple dipole pomeron amplitude proposed in [13] and containing two exponents with a dependence on the square of the transferred impulse, i.e., the diffraction cone of the differential cross-section is described by a combination of two exponents. To determine the model parameters within the framework of regression (numerical calculations), the least squares method will be used, which leads to equations whose solutions are these parameters. Using them, differential cross-sections in the vicinity of their minimum will also be calculated in comparison with experimental values. Parameter errors will be determined. Constraints on parameters will also be obtained, the implementation of which will be directly checked. The statistical acceptability of the model will also be determined.

Materials and Methods

In [13], it was shown that the amplitude of a dipole pomeron with two exponential dependences on the square of the transferred momentum in the centre of mass system for pp-scattering at high energies leads to the expression of a differential cross-section of the process that has extrema, including a minimum, as well as an experimental curve for each energy of available experiments. The trajectory of the pomeron is chosen so as not to break the unitarity, i.e., its intersept ($t=0$) equals 1: $\alpha(t)=1+\alpha' t$, where $\alpha'=0.266$ GeV^2, t is the square of the transferred impulse is specified. The amplitude has terms with independent parameters $a, b, c,$ which also affect the shape of the theoretical curve. It also has a common multiplier that sets its scale. The specified amplitude has the following form:

$$P(s,t) = isg_0[e^{at} + ce^{bt}\ln(-i\frac{s}{s_0})](-i\frac{s}{s_0})^{\alpha(t)-1} \quad (1)$$

where the Mandelstam variables are $s=(p_1+p_2)^2$ and $t=(p_1-p_3)^2$, p_1, p_2 are the proton initial four-impulses, p_3 is the four-impulse of a scattered proton, $s_0=1$ GeV^2, g_0 is the scale multiplier, a, b, c are the mentioned parameters.

In amplitude (1), unknown parameters are found using numerical calculations. To calculate the amplitude parameters from experimental data of differential cross-sections, the least squares method, which is widely used in statistics, is used, which searches for the minimum square of the difference between the theoretical and experimental values of a physical quantity. The system of three equations obtained using this method is solved by the rapid descent method [14], or otherwise by the gradient method. It was chosen because upon performing calculations in consecutive approximations, i.e., iterations, it quickly converges to a solution. This method reduces the amount of machine time upon calculations.

For compactness and convenience of solving a system of equations, it is written in matrix form. This allows creating simple and transparent programmes for finding approximate parameter values.

The equations themselves are transcendental, so they are solved approximately. This way, the parameters will have errors. To determine these errors, a covariance matrix is calculated, on the diagonal of which there are squares of standard deviation, i.e., squares of errors.

For day, experimental data for the differential cross-section of elastic pp-scattering at high energies exist at eight energies from 23.5 GeV to 13 TeV. The limitation of the model is that the proposed simple amplitude with three parameters is only an initial one for constructing more complex amplitudes. It is important that this

initial amplitude describes the minima of the specified cross-sections and their vicinity. However, this description for each energy can only be made with its own set of parameters.

As noted above, with a single set of parameter values, such description is possible with more complex amplitudes, which contain considerably more terms and, accordingly, many more parameters.

The complete set of parameters, which is an approximate set, is subject to added verification. It lies in obtaining an answer to whether the parameters satisfy the resulting general constraints, which are written as inequalities. If the result is positive, one can be sure that the accuracy of calculations is sufficient. Substituting parameters in the inequality showed that all of them are fulfilled, and the obtained values are quite far from the limit values of the constraints. Furthermore, the inequalities obtained earlier in [13] are also satisfied.

However, to find out the adequacy of the model, it is necessary to verify its statistical acceptability, which was done using the Fischer criterion [15]. This simple statistical method is widely used in the regressive analysis of experimental data by models, i.e., upon their theoretical explanation. All values of the Fischer quantile turned out to be less than the critical one, i.e., the model is statistically acceptable.

Results and Discussion

According to the least squares method, wherein the square of the difference between the experimental and theoretical values of a physical quantity reaches a minimum, the amplitude parameters a, b and c are found (1).

After differentiating the specified square by these parameters and equating the results with zero, a system of three equations (2.1-2.3) is obtained as follows:

$$\sum_{i=1}^{21}\left[(f_i)_{\text{exp}} - f_i\right]\frac{\partial f_i}{\partial a} = 0 \quad (2.1)$$

$$\sum_{i=1}^{21}\left[(f_i)_{\text{exp}} - f_i\right]\frac{\partial f_i}{\partial b} = 0 \quad (2.2)$$

$$\sum_{i=1}^{21}\left[(f_i)_{\text{exp}} - f_i\right]\frac{\partial f_i}{\partial c} = 0 \quad (2.3)$$

In equations (2.1-2.3) $(f_i)_{\text{exp}}$ – experimental values of these cross-sections at energies of 2.76, 7, 13 TeV [1-3], 23.5, 30.7, 44.7, 52.8 TV 62.5 GeV (for references to experimental data at these energies, see [5]) for the squared of transferred impulse t_i (10 on both sides of the minimum, except for the energy of 2.76 TeV, for which it was impossible to do this from the data available), f_i – their theoretical values (3). In Equation (3) $g=g_0 s_0$, w=0.3894 $mb{\cdot}GeV^2$ – transfer coefficient from units where $\hbar$=c=1, to mb/GeV^2.

$$f_i = f(s,t_i) = \frac{d\sigma(s,t=t_i)}{dt} = \frac{\pi g^2}{s^2} w\left[(e^{at_i} + ce^{bt_i}\ln\frac{s}{s_0})^2 + \left(\frac{\pi c}{2}\right)^2 e^{2bt_i}\right]\left(\frac{s}{s_0}\right)^{2\alpha(t_i)} \quad (3)$$

Expanded form of Equation (2.1-2.3) for real functions F_i, they will be written as follows (4-9):

$$F_1 = \sum_{i=1}^{21}\left[(f_i)_{\text{exp}} - f_i\right]\frac{\partial \tilde{f}_i}{\partial a} = 0 \quad (4)$$

$$F_2 = \sum_{i=1}^{21}\left[(f_i)_{\text{exp}} - f_i\right]\frac{\partial \tilde{f}_i}{\partial b} = 0 \quad (5)$$

$$F_3 = \sum_{i=1}^{21}\left[(f_i)_{\text{exp}} - f_i\right]\frac{\partial \tilde{f}_i}{\partial c} = 0 \quad (6)$$

where:

$$\frac{\partial \tilde{f}_i}{\partial a} = t_i e^{at_i}(e^{at_i} + ce^{bt_i}\ln s)s^{2\alpha' t_i} \quad (7)$$

$$\frac{\partial \tilde{f}_i}{\partial b} = t_i\left[ce^{bt_i}\ln s(e^{at_i} + ce^{bt_i}\ln s) + \left(\frac{\pi c}{2}\right)^2 e^{2bt_i}\right]s^{2\alpha' t_i} \quad (8)$$

$$\frac{\partial \tilde{f}_i}{\partial c} = \left[2\ln s(e^{at_i} + ce^{bt_i}\ln s)e^{bt_i} + \frac{\pi^2 c}{2}e^{2bt_i}\right]s^{2\alpha' t_i} \quad (9)$$

Functions F_i can be considered the elements of the matrix $\boldsymbol{F}$ (10):

$$F = \begin{pmatrix} F_1 \\ F_2 \\ F_3 \end{pmatrix} \quad (10)$$

To solve the system of Equations (4-6) according to the rapid descent method, as in [14], an auxiliary function is introduced as follows:

$$\Phi = F^T F = F_1^2 + F_2^2 + F_3^2 \quad (11)$$

where in expression (11) T is the matrix transposition sign. Values of parameters that are the solution of the equation Φ=0, are also solutions of the system of Equations (4-6).

On l^{th} step of successive approximations, solutions for parameters are obtained according to Formula (12):

$$A_{l+1} = A_l - \frac{F_l^T W_l W_l^T F_l}{(W_l W_l^T F_l)^T (W_l W_l^T F_l)} W F_l \quad (12)$$

where (13):

$$A = \begin{pmatrix} a \\ b \\ c \end{pmatrix} \quad (13)$$

while the Jacobi matrix (14)

$$W = \begin{pmatrix} \frac{\partial F_1}{\partial a} & \frac{\partial F_1}{\partial b} & \frac{\partial F_1}{\partial c} \\ \frac{\partial F_2}{\partial a} & \frac{\partial F_2}{\partial b} & \frac{\partial F_2}{\partial c} \\ \frac{\partial F_3}{\partial a} & \frac{\partial F_3}{\partial b} & \frac{\partial F_3}{\partial c} \end{pmatrix} \quad (14)$$

The elements of matrix (14) have the form (15-23):

$$\frac{\partial F_1}{\partial a} = \sum_{i=1}^{21}\left[-\frac{\partial f_i}{\partial a}\frac{\partial \tilde{f}_i}{\partial a} + \left((f_i)_{\text{exp}} - f_i\right)\frac{\partial^2 \tilde{f}_i}{\partial a^2}\right] \quad (15)$$

$$\frac{\partial F_1}{\partial b} = \sum_{i=1}^{21}\left[-\frac{\partial f_i}{\partial b}\frac{\partial \tilde{f}_i}{\partial a} + \left((f_i)_{\text{exp}} - f_i\right)\frac{\partial^2 \tilde{f}_i}{\partial a \partial b}\right] \quad (16)$$

$$\frac{\partial F_1}{\partial c} = \sum_{i=1}^{21}\left[-\frac{\partial f_i}{\partial c}\frac{\partial \tilde{f}_i}{\partial a} + \left((f_i)_{\text{exp}} - f_i\right)\frac{\partial^2 \tilde{f}_i}{\partial a \partial c}\right] \quad (17)$$

$$\frac{\partial F_2}{\partial a} = \sum_{i=1}^{21}\left[-\frac{\partial f_i}{\partial a}\frac{\partial \tilde{f}_i}{\partial b} + \left((f_i)_{\text{exp}} - f_i\right)\frac{\partial^2 \tilde{f}_i}{\partial a \partial b}\right] \quad (18)$$

$$\frac{\partial F_2}{\partial b} = \sum_{i=1}^{21}\left[-\frac{\partial f_i}{\partial b}\frac{\partial \tilde{f}_i}{\partial b} + \left((f_i)_{\text{exp}} - f_i\right)\frac{\partial^2 \tilde{f}_i}{\partial b^2}\right] \quad (19)$$

$$\frac{\partial F_2}{\partial c} = \sum_{i=1}^{21}\left[-\frac{\partial f_i}{\partial c}\frac{\partial \tilde{f}_i}{\partial b} + \left((f_i)_{\text{exp}} - f_i\right)\frac{\partial^2 \tilde{f}_i}{\partial b \partial c}\right] \quad (20)$$

$$\frac{\partial F_3}{\partial a} = \sum_{i=1}^{21}\left[-\frac{\partial f_i}{\partial a}\frac{\partial \tilde{f}_i}{\partial c} + \left((f_i)_{\text{exp}} - f_i\right)\frac{\partial^2 \tilde{f}_i}{\partial a \partial c}\right] \quad (21)$$

$$\frac{\partial F_3}{\partial b} = \sum_{i=1}^{21}\left[-\frac{\partial f_i}{\partial b}\frac{\partial \tilde{f}_i}{\partial c} + \left((f_i)_{\text{exp}} - f_i\right)\frac{\partial^2 \tilde{f}_i}{\partial b \partial c}\right] \quad (22)$$

$$\frac{\partial F_3}{\partial c} = \sum_{i=1}^{21}\left[-\frac{\partial f_i}{\partial c}\frac{\partial \tilde{f}_i}{\partial c} + \left((f_i)_{\text{exp}} - f_i\right)\frac{\partial^2 \tilde{f}_i}{\partial c^2}\right] \quad (23)$$

Errors in the values of parameters (13) that occur when solving equations (4-6) are obtained from the diagonal elements of the covariance matrix [15]. This matrix has the following form (24):

$$B = S^2 R^{-1}, \quad R^{-1} = -\mu W^T \quad (24)$$

where S^2 is the estimated value of the square of the standard deviation σ^2, μ is the multiplier before $\boldsymbol{WF}_l$ in Formula (12).

This is the estimated value of [15] (25):

$$S^2 = \frac{Q_{min}}{n-m} \quad (25)$$

where n is the number of experimental data used in calculations, m is the number of parameters. Value Q_{min} by definition (26):

$$Q_{min} = \sum_{i=1}^{21}(\xi_i - \tilde{y}_i)^2 = (\xi - \tilde{y})^T(\xi - \tilde{y}) \quad (26)$$

where $\boldsymbol{\xi}$ is the column of experimental values of differential cross-sections, $\tilde{y}$ is the column of theoretical values (3) of these cross-sections when found g, a, b, c.

By entering a matrix-column $\boldsymbol{\Delta\xi}$, elements of which are $\boldsymbol{\Delta}\xi_i = x_i - f_i$, and using the decomposition by parameters at a fixed energy, the following expression (27) is obtained:

$$\xi_i - f(t_i, \tilde{A}) = \xi_i - y_i - \sum_{k'=1}^{m}\frac{\partial f(t_i, A)}{\partial A_{k'}}\left(\tilde{A}_{k'} - A_{k'}\right) + \ldots = \Delta\xi_i - \sum_{k'=1}^{m} D_{ik'}\,\Delta A_{k'} + \ldots \quad (27)$$

where $y_i = \xi_i - f(t_i, \boldsymbol{A})$; $D_{ik} = \partial f(t_i, \boldsymbol{A})/\partial A_k$; $\Delta A_{k'} = \tilde{A}_{k'} - A_{k'}$; m – number of parameters.

After performing some transformations in (27), the following equation is obtained (28):

$$Q_{min} = \Delta\xi^T(E - WDR^{-1}D^T)W(E - DR^{-1}D^TW)\Delta\xi \quad (28)$$

where E is the unit matrix.

Together with experimental ones, Figures (1-8) demonstrate theoretical cross-sections in the vicinity of minima, which are calculated for the found values of parameters and the scale multiplier.

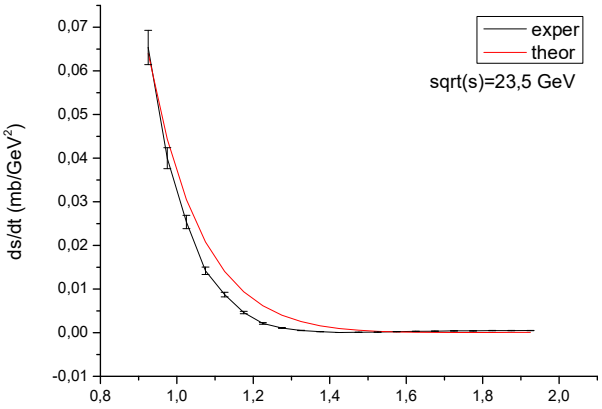

Figure 1. Differential cross-section elastic pp-scattering at √s= 23.5 GeV

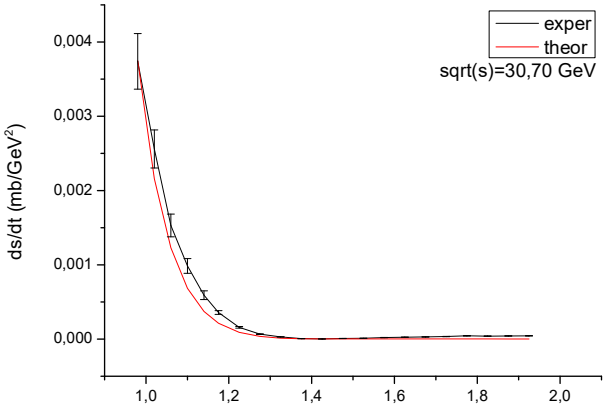

Figure 2. Differential cross-section of elastic pp-scattering at √s=30.7 GeV

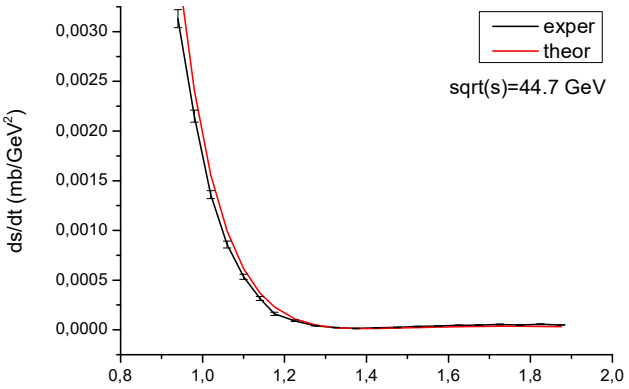

Figure 3. Differential cross-section elastic pp-scattering at √s= 44.7 GeV

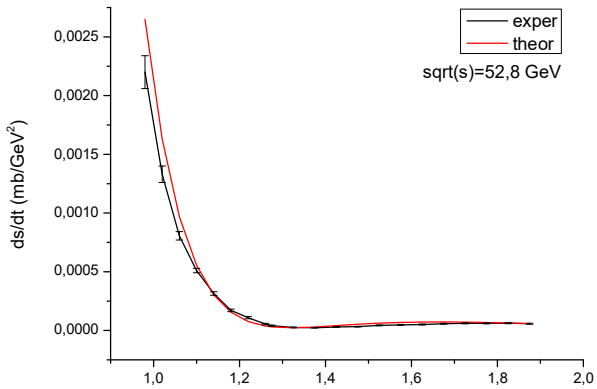

Figure 4. Differential cross-section of elastic pp-scattering at √s= 52.8 GeV

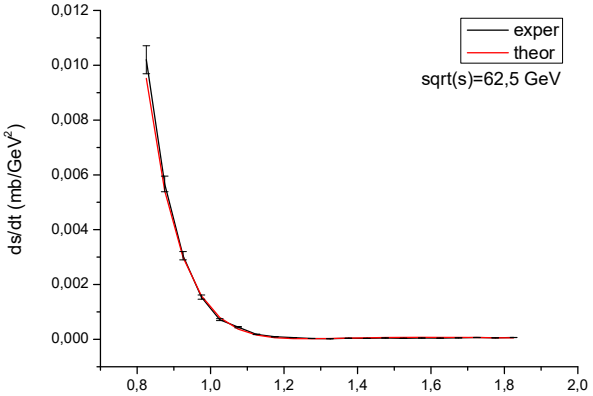

Figure 5. Differential cross-section elastic pp-scattering at √s= 62.5 GeV

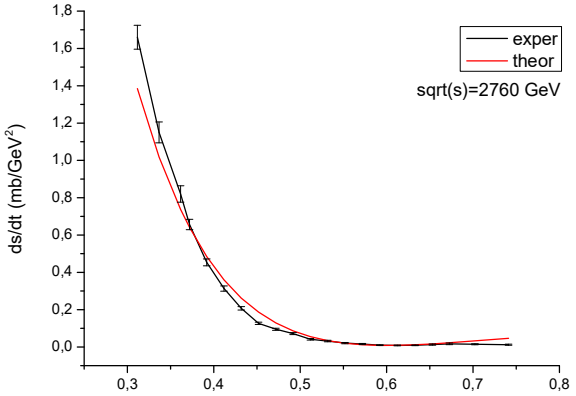

Figure 6. Differential cross-section of elastic pp-scattering at √s=2.76 GeV

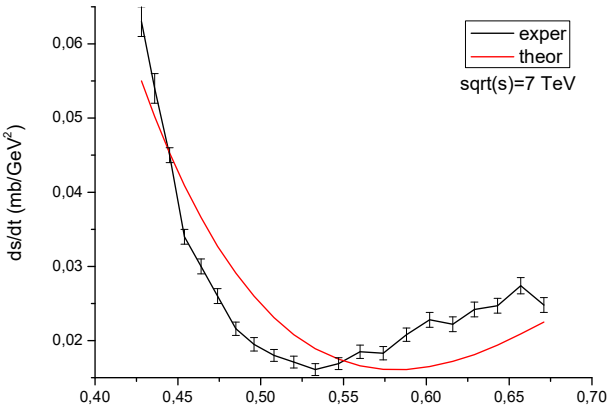

Figure 7. Differential cross-section elastic pp-scattering at √s=7 TeV

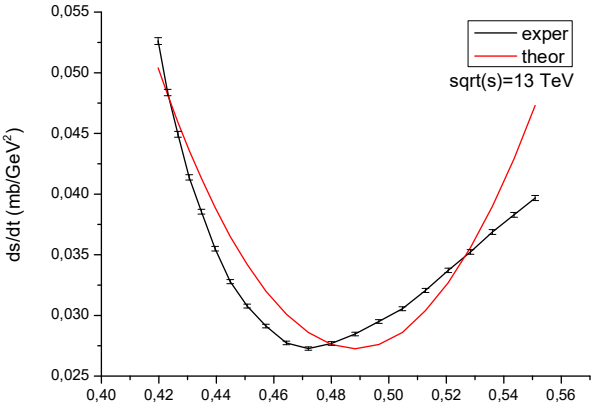

Figure 8. Differential cross-section of elastic pp-scattering at √s=13 TeV

As can be seen from the figures, the graphs of differential cross-sections of the model up to an energy of 2.76 TeV are in satisfactory agreement with the experimental data. Notably, the shapes of the theoretical curves for all energies are similar to the experimental ones, but Figures 6-8 demonstrate noticeable shifts between them, but not in all sections of the curves. This means that in these cases, the parameters found were farther from their exact values, which exist only theoretically. The cross-sections in Figures 1-5 turned out to be the closest to the experimental ones, i.e., better parameters were found here than in earlier cases. The quality of parameters depends on the choice of their zero approximation upon solving equations. While this initial choice is quite arbitrary. The worst agreement with the experiment is observed at 7 TeV. But in this case, the experimental errors are also much larger than at other energies. The need to improve the statistics of this experiment is drawn in the study [16]. However, the experiment for *pp*-scattering at 7 TeV has not yet been repeated. In models with a larger number of parameters, a better match with the experiment can be achieved.

The values of the scale multiplier and model parameters obtained from equations (2-4) are shown in Table 1. Table 1 also demonstrates the parameter errors calculated using the covariance matrix (24). They are insignificant, except for the parameter **c** at energies of 2.76, 7, and 13 TeV, for which they are 8.5%, 7.0%, and 4.4%, respectively.

Table 1. Values of the scale multiplier and parameters at different energies

No.	$\sqrt{s}$, GeV	g	a, GeV^{-2}	b, GeV^{-2}	c
1.	23.5	0.254	-0.3739±0.001	1.3990±0.004	-3.148±0.001
2.	30.7	0.3004	0.9523±0.002	3.95±0.005	-10.10±0.005
3.	44.7	1.138	0.645±0.00001	-0.562±0.000004	-0.01927±0.0003
4.	52.8	0.1823	-0.512±0.001	1.9365±0.002	-2.981±0.0007
5.	62.5	0.1763	-0.5436±0.0004	2.0406±0.001	-2.9406±0.0005
6.	2760	1.930	-2.8607±0.0010	-0.6804±0.0017	-0.2354±0.020
7.	7000	2.3825	-3.65±0.0002	-2.901±0.0002	-0.08563±0.006
8.	13000	1.536	-5.3738±0.0002	-4.2338±0.0002	-0.0912±0.004

In [13], a constraint on the parameters a, b, c was obtained provided that $a>0$, $b<0$, which is not common. The following is a constraint for arbitrary valid values a and b. Recall that the solution $x=e^{(a-b)t}$ (expression (9) for equation (10) in [13]) is a positive number, i.e., only positive solutions of the quadratic equation are considered. General view of such equation (29):

$$px^2+qx+r=0 \qquad (29)$$

Positive solutions are obtained in the following cases (30):

$$p>0,\ -q+\sqrt{q^2-4pr}>0,$$
$$p>0,\ -q-\sqrt{q^2-4pr}>0,$$
$$p<0,\ -q+\sqrt{q^2-4pr}<0,$$
$$p<0,\ -q-\sqrt{q^2-4pr}<0$$

For equation (10) in [13] $p=a+\alpha' L$, $q=-|c|L(a+b+2\alpha' L)$, $r=c^2(b+\alpha' L)(L^2+\pi^2/4)$, $L=\ln(s/s_0)$]. Thus, for the parameters a, b, c four groups of constraints are obtained (31.1-31.4):

1) $p>0$, $q>0$, $r<0$; $a>0$, $b< -(a+2\alpha' L)$; $-\alpha' L<a<0$, $b<-\alpha' L$, $b<|a|-2\alpha' L$;
2) $p>0$, $q<0$, $r<q^2/4p$; $a>0$, $b> -(a+2\alpha' L)$, $(b+\alpha' L)(L^2+\pi^2/4)< <L^2(a+b+2\alpha' L)^2/4(a+\alpha' L)$; $-\alpha' L<a<0$, $b>|a|-2\alpha' L$, $(b+\alpha' L)(L^2+\pi^2/4)<L^2(a+b+2\alpha' L)^2/4(a+\alpha' L)$ (31.1)

$p>0$, $q<0$, $r>0$; $-\alpha' L<a<0$, $b>-\alpha' L$, $b>|a|-2\alpha' L$; (31.2)

$p<0$, $q>0$, $-\alpha' L<a<0$, $b<-\alpha' L$, $b<|a|-2\alpha' L$); (31.3)

$p<0$, $q<0$, $r>0$; $-\alpha' L<a<0$, $b>-\alpha' L$, $b>|a|-2\alpha' L$ (31.4)

Table 2 demonstrates the calculated coefficients of quadratic equation (29).

Table 2. Values of the coefficients of equation (29) and its discriminant factor

1.	$\sqrt{s}$, GeV	$\ln(s/s_0)$	p, GeV^{-2}	q, GeV^{-2}	r, GeV^{-2}	($p>0$), ($r<$) $q^2/4p$, GeV^{-2}
2.	23.5	6.3140	1.3056	-87.1414	1,291.52	1,454.05
3.	30.70	6.8485	2.7740	-591.1049	29,067.25	31,489.28
4.	44.7	7.5999	2.6666	-0.6043	0.0326	0.0342
5.	52.8	7.9330	1.5982	-133.4911	2,351.80	2,787.49
6.	62.5	8.2703	1.6563	-143.4081	2,598.50	3,104.19
7.	2,760	15.8460	1.3543	-18.2366	49.66	61.39
8.	7,000	17.7073	1.0601	-4.3508	4.19	4.46
9.	13,000	18.9454	-0.3343	-0.8144	2.42	–

In this table, for the collision energies at the found values of the parameters, the coefficients of equation (29) are given and for $p>0$ factor that is included in the discriminant. Since all r are positive, then for (unique) $p<0$, the discriminant is always positive, i.e., it does not give any restriction on the coefficients. For the complete set of parameter values, the coefficient q turned out to be negative, this reduces the number of resulting irregularities that need to be verified. This also applies to inequalities for which $r<0$.

Further, Table 3 demonstrates the calculated corresponding parts of the inequalities, which include the model parameters.

Table 3. Calculated values of the expressions from inequalities (31.1, 31.2, 31.4) and inequality (23) from the study [13] for the corresponding values of parameters *a, b* and *c*

, GeV	(*p*>0) *a*>0	*b*	(*b*>) -(*a*+2*α'L*)	(*b*+*α'L*)(*L*²+*π*²/4)<*L*² (*a*+*b*+2*'L*)²/4(*a*+*'L*), GeV⁻²	
	(31.1), 2)				
30.70	0.9523	3.95	-4.5957	284.9<308.8	
44.7	0.645	-0.562	-4.6881	87.9<92.2	
	(p>0) a<0	b5	(b>) |a|-2α'L	(b+α'L)(L²+π²/4)<L²(a+ +b+2α'L)²/4(a+α'L)	
23.5	-0.3739	1.3990	-2.9851	130.33<146.72	
52.8	-0.512	1.9365	-3.7084	264.65<313.69	
62.5	-0.5436	2.0406	-3.8562	300.50<358.98	
2760	-2.8607	-0.6804	-5.5694	896.25<1107.88	
7000	-3.65	-2.901	-5.7703	571.72<608.73	
	(31.2)				
	(p>0) a<0	*b12*	-α'L (<a<0)	(b>) |a|-2α'L	
23.5	-0.3739	1.3990	-1.6785	-2.9830	
52.8	-0.512	1.9365	-2.1094	-3.7068	
62.5	-0.5436	2.0406	-2.1998	-3.8060	
2760	-2.8607	-0.6804	-4.2161	-5.5715	
7000	-3.65	-2.901	-4.7109	-5.7715	
	(31.4)				
	(p<0), a (<0)	b19	(a<) -α'L	(b>) -α'L	(b>) |a|-2α'L
13000	-5.3738	-4.2338	-5.0395	-5.0395	-4.7052
	a	*b*	*c*	*(πα'/2√a)²*	*4a/(πc)²*
44.7	0.645	-0.562	-0.01927	0.2707	703.97

Table 3 shows numerical calculations of inequalities (31.1, 31.2) and (31.4), and from (31.1) only the second part was to be calculated. This is marked in the second line. The reason is related to the signs of the coefficients of the quadratic equation, as already explained in the previous paragraph. The same reason for the lack of inequality analysis (31.3).

The first column of the table contains the values of the collision energies, and the second and third columns contain the values of the parameters *a* and *b*. In the fourth column up to end including the twentieth row, the calculated values of the left or right parts of the corresponding inequalities are given, and in parentheses — the parameters that relate to the constraint. Similarly, the fifth column shows the values of the left and right sides of the corresponding inequalities.

The last two rows of the table represent the results of calculations of inequality (23) obtained in [13] with parameter constraints not under general conditions.

Table 3 demonstrates that for the entire set of parameters *a, b* and *c* the inequalities are met. Notably, for the corresponding *a* and *b,* the inequality (21) from [13] is also performed: a | b |>$(\pi\alpha'/2)^2$=0.15.

The possibility of using the model for further generalisations is determined according to the Fischer criterion [15]. It is characterised by the correlation of the remaining amount to the recovery amount. The first sum considers the errors of calculations based on the theoretical model, where there are both experimental errors and errors from an approximate solution of equations, and the second – only experimental errors. The Fischer quantile is calculated according to the formula (32):

$$F = \frac{\sum_{i=1}^{21}\left[(f_i)_{\text{exp}} - f(s,t_i)\right]^2}{\sum_{i=1}^{21}\left[(f_i)_{\text{exp}} - \bar{f}_{\text{exp}}\right]^2}\frac{n}{m} \qquad (32)$$

where f_{exp} is the average value of the experimental data sample, m is the number of parameters, n is the number of selected experimental points. The resulting quantiles are presented in Table 4.

Table 4. Value of Fischer quantiles for collision energies

	$\sqrt{s}$, GeV	F	Tabular value of F for m=3, n=21 with a probability of 95% [15]
1	23.5	0.030	3.07
2	30.70	0.020	
3	44.7	0.068	
4	52.8	0.049	
5	62.5	0.0043	
6	2,760	0.37	
7	7,000	0.036	
8	13,000	0.0072	

In Table 4 for high energies at which there are experimental data of differential cross-sections of elastic *pp*-scattering represented is calculated according to the Fischer quantile formula (31). The sample average for each energy is the arithmetic mean of 21 experimental points, which was used in calculating the parameters. The third column shows that with the most used 95% confidence in practice, Fischer quantiles are less than the critical value. Thus, the model is statistically acceptable.

Conclusions

In the amplitude of elastic *pp*-scattering, which contains a dipole pomeron with a linear trajectory and its intersept equals 1, and the diffraction cone of the differential cross-section is described by two exponents, the values of the parameters and the scaling factor were found by the regression method involving the least squares method. With these values, the differential cross-sections around their minima were calculated for eight energies. They coincide better with the experiment at energies from 23.5 to 62.5 GeV than for energies of 2.76, 7, and 13 TeV. The difference between the experiment and the theory at an energy of 7 TeV is quite noticeable. This is primarily due to considerably larger experimental errors than in other experiments. The proximity of the theory to the experiment characterises the quality of the found parameters, which in numerical calculations largely depends on the successful choice of their initial values upon iteration. On the other hand, such a simple amplitude, which is only primitive for constructing a complex one containing more than 20 parameters, cannot give such a qualitative description as a complex one.

The errors of the parameters were calculated, which turned out to be small. This indicates a sufficient number of consecutive approximations upon performing calculations.

The constraints that the parameters must meet are found. Substituting them into constraint expressions showed that the inequalities hold. This also indicates sufficient accuracy of calculations.

As a result of verifying the statistical acceptability of the model using the Fischer method, it turned out to be positive. Thus, the amplitude considered in the article with the found parameters can be basic in the construction of complex amplitudes for describing a wider range of physical quantities in *pp*-scattering.

References

[1] Antchev G, Aspell P, Atanassov I, Avati V, Baechler J, Berard V, et al. Elastic differential cross-section dσ/dt at √s=2.76 TeV and implications on the existence of a colourless C-odd three-gluon compound state. *European Physical Journal C*. 2020;(80):91-1–91-10.

[2] Antchev G, Aspell P, Atanassov I, Avati V, Baechler J, Berard V, et al. Measurement of proton-proton elastic scattering and total cross-section at √s=7 TeV. *Europhys. Lett.* 2013;101:21002-1–21002-8.

[3] Antchev G, Aspell P, Ciesielski R, Avati V, Baechler J, Baldenegro C, et al. Elastic differential cross-section measurement at √s=13 TeV by TOTEM. *European Physical Journal C.* 2019;(79): 861-1–861-20.

[4] Jenkovszky L, Schicker R, Szanyi I. Elastic and diffractive scatterings in the LHC era. *International Journal of Modern Physics E.* 2018;(27):1830005-1–1830005-44.

[5] Bence N, Lengyel A, Tarics Z, Martynov E, Tersimonov G. Froissaron and Maximal Odderon with spin-flip in pp and high energy elastic scattering. *European Physical Journal A.* 2021;(57):265-1–265-11.

[6] Shabelski YuM, Shuvaev AG. Unified description of LHC data on elastic pp scattering. *Modern Physics Letters A.* 2019;(33):1950305-1–19530507.

[7] Martynov E, Nicolescu B. Odderon effects in the differential cross-sections at Tevatron and LHC energies. *European Physical Journal C.* 2019;(79);461-1–461-14.

[8] Hagiwara Y, Hatta Y, Pasechnik R, Zhou J. Spin-dependent Pomeron and Odderon in elastic proton-proton scattering. *European Physical Journal C.* 2020;(80):427-1–427-19.

[9] Kopeliovich BZ, Krelina M, Potashnikova IK. Probing the Pomeron spin structure with Coulomb-nuclear interference. *Physical Letters B.* 2021;(816):136262-1–136262-6.

[10] Campos SD. An approach to the leading Regge pole. *Physica Scripta.* 2020;(95):065302-1–065302-10.
[11] Broilo M, Fagundes DA, Luna EGS, Peláez M. Soft Pomeron in light of the LHC correlated data. *Physical Review D.* 2021;(103):014019-1–014019-15.
[12] Godizov AA. High-energy elastic diffractive scattering of nucleons in the framework of the two-Reggeon eikonal approximation (from U-70 to LHC). *European Physical Journal C.* 2022;(82):56-1–56-13.
[13] Tarics ZZ. On the question of minima and maxima in differential sections of elastic proton-proton scattering at high energies. *Scientific Herald of Uzhhorod University. Series "Physics".* 2006;(19):176-80.
[14] Demidovich BP, Maron IA. Fundamentals of computational mathematics. Third edition, cor. Moscow: Science; 1966. 664 p.
[15] Lavrenchik VN. Setting up a physical experiment and statistical processing of its results. Kyiv: Publishing House Energoatom; 1986. 272 p.
[16] Jenkovszky L, Szanyi I. Structures in the diffraction cone: The "break" and "dip" in high-energy proton-proton scattering. *Mod. Phys. Lett.* 2017;(32):1750116.

Проста модель для опису околу мінімуму диференціального перерізу пружного розсіяння протонів на протонах за високих енергій

Норберт Йосипович Бенце[1], Олександр Іванович Лендєл[2], Золтан Золтанович Торич[2]

[1]Ужгородський національний університет
88000, вул. Університетська, 14, м. Ужгород, Україна

[2]Інститут електронної фізики НАН України
88017, вул. Університетська, 21, м. Ужгород, Україна

Анотація

Актуальність. Найсучаснішою і широко застосованою феноменологічною теорією, яка добре описує цілий спектр фізичних характеристик таких процесів як пружне і непружне протон-протонне та антипротон-протонне розсіяння за високих енергій, є метод полюсів Редже в релятивістській теорії. Виходячи з простої амплітуди, наприклад дипольної померонної, де померон є полюсом Редже, дослідники додають до неї різні члени. За допомогою таких складніших амплітуд вдається добре або задовільно пояснити разом не тільки експериментальні дані для згаданих реакцій, отримані в кінці минулого століття, але й останні, одержані на Великому адронному колайдері.

Мета. Метою статті є знаходження чисельних значень параметрів амплітуди, при яких задовільно описуються околи мвнімумів диференціальних перерізів пружного розсіяння протонів на протонах за високих енергій, а також відповіль на питання, чи задовольняють параметри отриманим обмеженням.

Методи. Для знаходження параметрів амплітуди використано метод найменших квадратів і отримано рівняння мінімумів для квадратів різниць між експериментальними та теоретичними значеннями зазначених перерізів. Ці рівняння трансцентдентні, тому розв'язуються наближенню. В рамках послідовних наближень вибрано метод, який забезпечує швидку збіжність процесу, а саме: метод скорішого спуску або градієнтний метод. Похибки параметрів обчислено за допомогою коваріаційної матриці. Статистична прийнятність моделі визначено за критерієм Фішера.

Результати. Чисельними розрахунками з експериментальних даних диференціальних перерізів пружного *pp*-розсіяння знайдено значення параметрів і масштабного множника амплітуди. За амплітудою в околі мінімумів обчислено диференціальні перерізи. Представлено відповідні графіки цих перерізів. Збіг з експериментом в більшості випадків задовільний, в окремих – якісний. Отримано коваріаційну матрицю, з якої знайдено похибки параметрів моделі. При загальних умовах виведено обмеження на знайдені наближені значення параметрів. Показано, що вони обмеженням задовольняють. За критерієм Фішера виконано перевірку статистичної прийнятності моделі, що виявилася позитивною

Висновки. Запропонована проста амплітуда забезпечує виконання обмеження Фруассара та унітарності. Вона служитиме як затравальна для побудови більш складних амплітуд, що описуватимуть широке коло експериментів протон-протонного й антипротон-протонного розсіянь за високих енергій

Ключові слова: амплітуда, параметр, дипольний померон, коваріаційна матриця